Supporting Information

Machida *et al.* 10.1073/pnas.0807390106

SI Methods

Cells. Huh7 cells were plated at 3×10^5 or 2×10^6 cells per 6-well or 10-cm dish and transfected with expression plasmids and a reporter construct.

Histology and Immunohistochemistry. Mouse livers from different genetic and treatment groups were fixed in neutral-buffered 4% paraformaldehyde at 4°C and processed for paraffin embedding. Five-micrometer sections were stained with hematoxylin and eosin. Immunohistochemistry staining of cryosections or paraffin sections was performed by using antibodies against TLR4 (HTA125; eBioscience), phospho-JNK (Santa Cruz Biotechnology), phospho-IκB (Cell Signaling Technology), TNF-α (RM9011; CALTAG), or Nanog (Abcam) based on the standard protocol with mounting media, including DAPI for nuclei counterstaining (Vector Laboratories), according to the manufacturer's recommendations.

Human Subjects. Necropsy liver tissues from patients with HCV infection with or without a history of alcoholism were obtained as cryopreserved samples according to the approved Institutional Review Board protocol. The samples were carefully screened for coinfection with other hepatitis virus or HIV as determined by serological tests, drug addiction, and comorbidities other than alcoholism as tested by clinical laboratory tests, and such samples were excluded from the study. Necropsy liver specimens from 8 HCV infected patients were examined for immunohistochemistry and immunoblat analysis. Four patients had a history of having more than 4 drinks per day for more than 15 years. The other 4 patients reportedly consumed alcohol only occasionally in a very moderate amount. They were all male with ages of 27≈59 years, but no information on smoking was avaialble. Histologically, they all had a varying degree of steatosis (microvesicular and macrovesicular) and inflammation, and these changes were more pronounced in alcohol-consuming HCV patients. Frozen necropsy liver tissues from patients with stroke but without apparent liver pathology were also obtained for immunoblotting.

Gene Array Analysis of Liver Tumors. For gene profiling, the Affymetrix mouse gene chip (GeneChip Mouse Genome 430A 2.0) was used, and analysis was performed in the Genome Core Facility at Los Angeles Children's Hospital. We performed microdissection to collect hepatocytes from NS5A Tg mice fed alcohol and wild-type (WT) mice fed alcohol for 12 months (14 months old). We prepared serial cryosections from 5 mice (3 males and 2 females) from each group, stained them with H&E, and collected hepatocytes from non-tumor-bearing areas using laser-capture microscopy as described previously (1–3). A minimum of 100≈200 cells were collected from each of 5 animals in both groups, and RNA individually extracted was pooled for each group for the analysis (1, 2, 4–6). Three different batches of RNA from different areas were prepared and used for microarray analysis. For gene profiling analysis, the Affymetrix mouse gene chip (GeneChip Mouse Genome 430A 2.0) was used in the Genome Core Facility at Los Angeles Children's Hospital. Data analysis was performed by using Partek Pro 5.1 (Partek Inc.). The normalization of the array data and statistical analysis were performed as described previously (7–9).

Plasmids, Lentivirus, and Retrovirus Vectors. The NS5A expression plasmid was constructed by inserting HCV NS5A cDNA behind the CMV promoter in pCDNA3.1 (Invitrogen). Lentivirus vectors were prepared by standard procedures in HEK293T cells. Three plasmids, packaging vector pPAX2 (Addgene), ecotropic envelope gene expression vector pMDV (Addgene), and the cassettes of shRNA were transfected in HEK293T cells by lipid-based transfection reagent FuGene6 (Roche). The retroviral expression vectors for shRNA of TLR4 and Nanog were obtained from Open Biosystems. Retrovirus expressing TLR4 was produced in Phoenix cells (10). After 72 hours of transfection, the virus supernatants were harvested and mixed with polybrene (4 μg/mL) and used to infect Huh7 cells. More detailed states of the patients are depicted in *SI Methods*.

Statistical Analysis. Statistical analysis of the data in Tables S1–S3 was performed by the χ^2 test or Student's t test. Values of $P < 0.05$ were considered to be statistically significant.

SI Discussion

One potential concern about the NS5A Tg used for the present study is that the protein may be overexpressed beyond the physiological range in chronic HCV infection, rendering artificial effects in the model. However, our immunoblot analysis comparing NS5A expression in livers of HCV patients and NS5A mice reveals NS5A expression in patient samples at the level approximating one third of the mouse Tg expression. Therefore, the NS5A expression in our model does not appear to be too excessive or unphysiological. In natural HCV infection, other viral proteins are also expressed and they may have interactive effects. Obviously, our animal model does not reproduce this environment as it is intended to specifically test the effects of the protein NS5A. In fact, because of this approach, we were able to reveal the novel roles of TLR4 and Nanog in their oncogenic potential in the context of the synergism specifically mediated by NS5A and alcohol. The roles of JNK and IKK in liver oncogenesis are important questions. AP-1 is activated in both HCC and chronic hepatitis (11). In vitro studies using liver-derived cell lines demonstrate rapid activation of AP-1 by HBV or HCV proteins (12). Our study also shows activation of JNK in alcohol-fed NS5A Tg mice in concurrence with the increased risk of liver tumors (Fig. S4). JNK-AP1 activation may induce compensatory cell proliferation via induction of growth factors such as IL-6, TNF-alpha, and HGF. This regenerative proliferation is considered as a predisposing condition for permanent oncogenic mutations in initiated hepatocytes for transmission to daughter cells (13–16). NF-kappaB activation protects the cells by induction of anti-apoptotic and anti-oxidant genes such as superoxide dismutase (SOD). Indeed, hepatocyte IKKβ inhibits liver carcinogenesis via attenuation of oxygen radical formation, and mice deficient in IKKβ are predisposed to JNK1-mediated oxidant stress and chemically induced liver tumors (13, 15). In our mouse model, NF-kappaB is activated by TLR4 signaling and this activation correlates with the expression of proinflammatory genes such as TNF-α. This pro-inflammatory response may also augment JNK-mediated hepatocellular damage and transformation. Our study did not address which isoform of JNK (JNK1/2) is responsible for NS5A-TLR4 mediated liver damage and oncogenesis, and this is an obvious question which will need to be addressed in future studies.

1. Marko-Varga G, Berglund M, Malmstrom J, Lindberg H, Fehniger TE (2003) Targeting hepatocytes from liver tissue by laser capture microdissection and proteomics expression profiling. *Electrophoresis* 24:3800–3805.
2. Michel C, *et al.* Liver gene expression profiles of rats treated with clofibric acid: comparison of whole liver and laser capture microdissected liver. (2003) *Am J Pathol* 163:2191–2199.
3. Espina V, Milia J, Wu G, Cowherd S, Liotta LA (2006) Laser capture microdissection. *Methods Mol Biol* 319:213–229.
4. Wulfkuhle JD, *et al.* (2002) Proteomics of human breast ductal carcinoma in situ. *Cancer Res* 62:6740–6749.
5. Wulfkuhle JD, Liotta LA, Petricoin EF (2003) Proteomic applications for the early detection of cancer. *Nat Rev Cancer* 3:267–275.
6. Espina V, *et al.* Protein microarrays: Molecular profiling technologies for clinical specimens. (2003) *Proteomics* 3:2091–2100.
7. Storey JD, Tibshirani R (2003) Statistical significance for genomewide studies. *Proc Natl Acad Sci USA* 100:9440–9445.
8. Sitkiewicz I, Musser JM (2006) Expression microarray and mouse virulence analysis of four conserved two-component gene regulatory systems in group a streptococcus. *Infect Immun* 74:1339–1351.
9. Graham MR, *et al.* (2005) Group A streptococcus transcriptome dynamics during growth in human blood reveals bacterial adaptive and survival strategies. *Am J Pathol* 166:455–465.
10. Saitoh S, *et al*. (2004) Lipid A antagonist, lipid IVa, is distinct from lipid A in interaction with Toll-like receptor 4 (TLR4)-MD-2 and ligand-induced TLR4 oligomerization. *Int Immunol* 16:961–969.
11. Liu P, *et al*. (2002) Activation of NF-kappa B, AP-1 and STAT transcription factors is a frequent and early event in human hepatocellular carcinomas. *J Hepatol* 37:63–71.
12. Kato N, *et al*. (2000) Activation of intracellular signaling by hepatitis B and C viruses: C-viral core is the most potent signal inducer. *Hepatology* 32:405–412.
13. Sakurai T, *et al*. (2008) Hepatocyte necrosis induced by oxidative stress and IL-1 alpha release mediate carcinogen-induced compensatory proliferation and liver tumorigenesis. *Cancer Cell* 14:156–165.
14. Eferl R, *et al*. (2003) Liver tumor development. c-Jun antagonizes the proapoptotic activity of p53. *Cell* 112:181–192.
15. Sakurai T, Maeda S, Chang L, Karin M (2006) Loss of hepatic NF-kappa B activity enhances chemical hepatocarcinogenesis through sustained c-Jun N-terminal kinase 1 activation. *Proc Natl Acad Sci U S A* 103:10544–10551.
16. Maeda S, Kamata H, Luo JL, Leffert H, Karin M (2005) IKKbeta couples hepatocyte death to cytokine-driven compensatory proliferation that promotes chemical hepatocarcinogenesis. *Cell* 121:977–990.

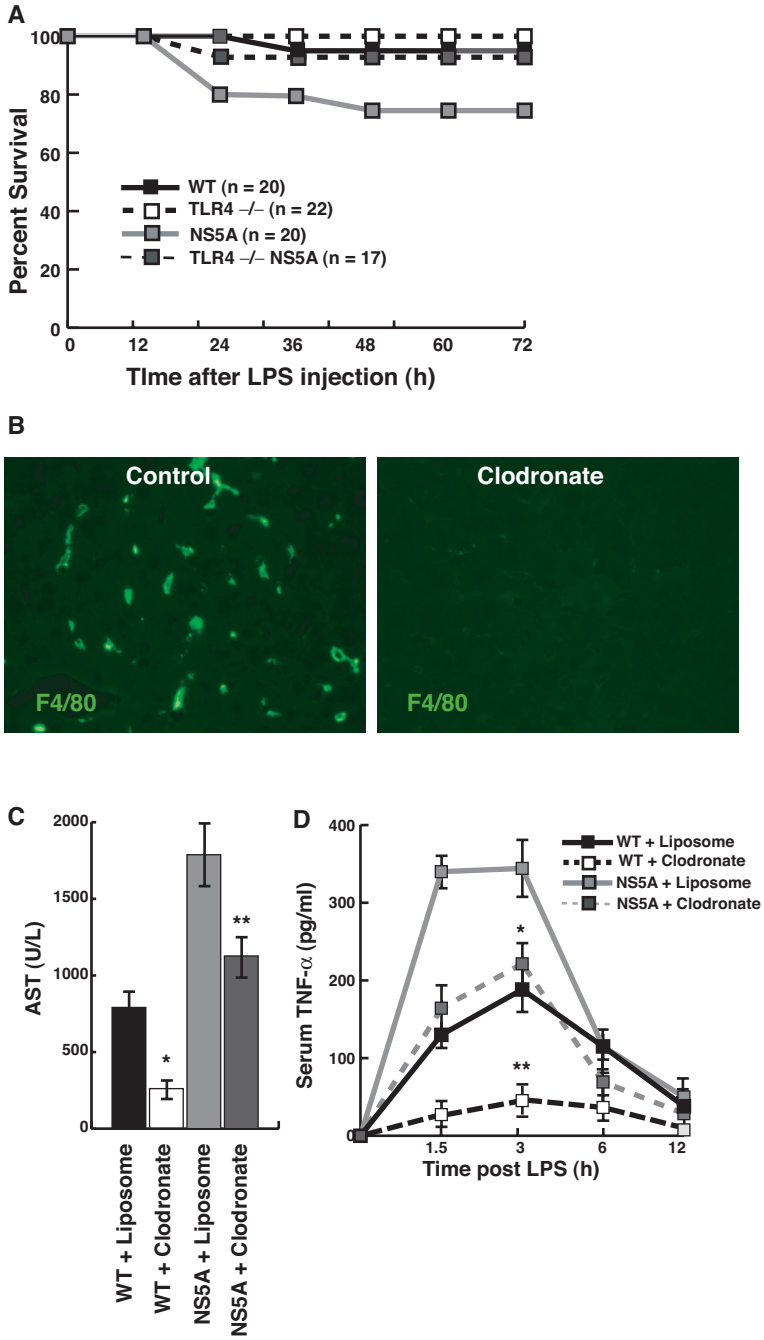

Fig. S1. Kupffer cell depletion only partially reduces LPS-induced TNF-α and liver damage in NS5A Tg mice. (*A*) Kaplan–Meier survival curves of wild-type (WT) and NS5A Tg mice in the presence or absence of *Tlr4*$^{-/-}$ after sublethal LPS challenge (25 mg/kg weight, intraperitoneal injection). NS5A Tg mice were susceptible to LPS-induced mortality compared with WT or Tlr4$^{-/-}$NS5A mice ($P < 0.01$, log-rank test). (*B*) Liposome-encapusulated Clodronate efficiently eliminated mouse Kuppfer cells. Note Kupffer cells stained with antibodies against F4/80 were almost completely eliminated by Clodronate compared with control liposome-injected mouse liver. (*C* and *D*) Mice were injected with liposome-encapsulated Clodronate or control liposomes, 2 days later challenged with a sublethal dose of LPS (25 mg/kg weight, intraperitoneal injection), and observed for 72 h. Serum AST levels were determined at 24 h after LPS injection (*C*), and serum TNF-α levels were monitored at 1.5≈12 h after LPS challenge (*D*). LPS-induced elevations of AST and TNF-α were largely (75≈80%) prevented by Clodronate pretreatment in WT mice. In contrast, the same treatment attenuated the same parameters only by 35≈39% in NS5A Tg mice. (*C*: *, $P < 0.004$ compared with NS5A given control liposomes, **, $P < 0.03$ compared with WT given control liposomes; *D*: *, $P < 0.03$ compared with NS5A given control liposomes, **, $P < 0.007$ compared with WT given control liposomes).

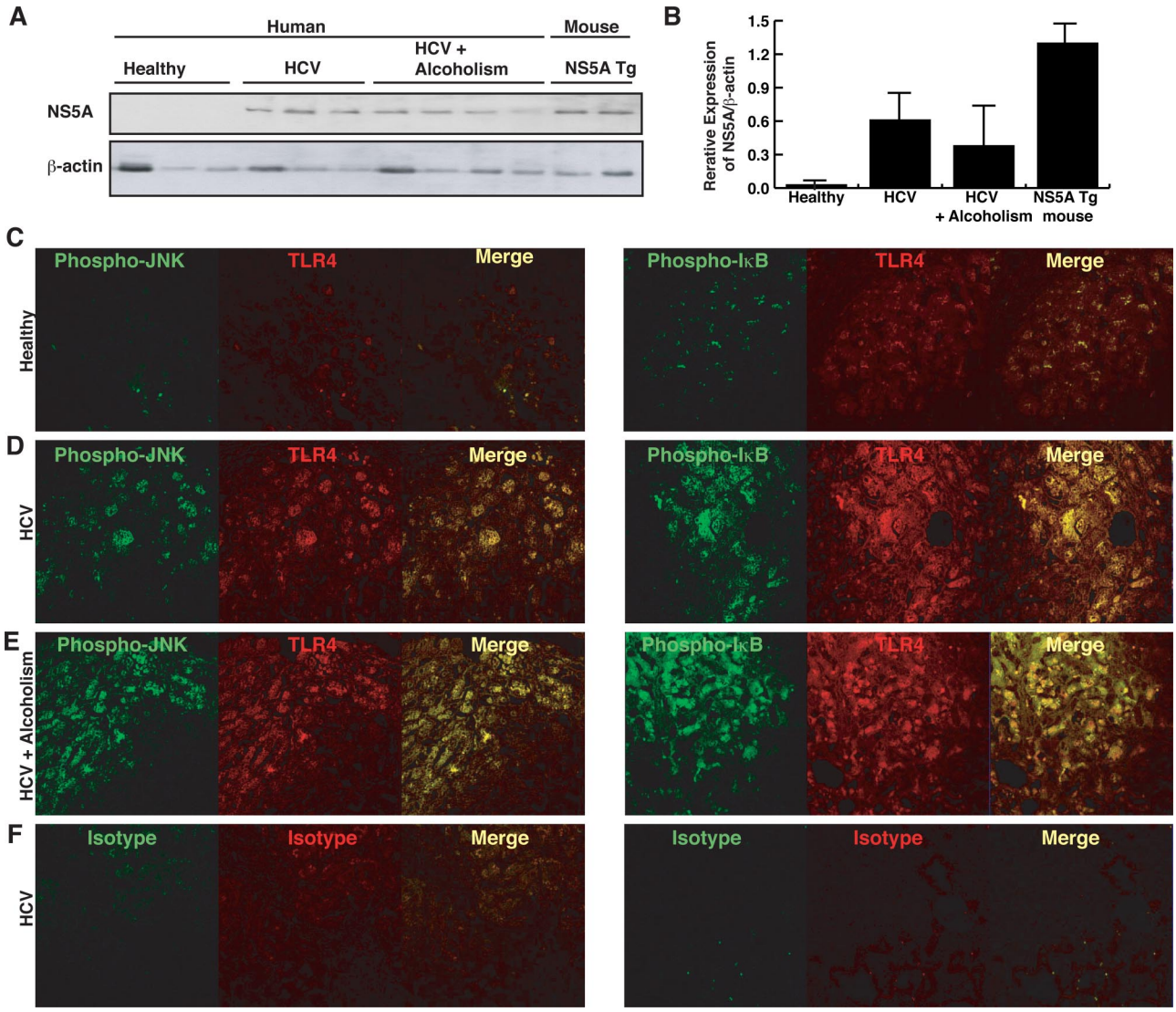

Fig. S2. NS5A and TLR4 induction in alcoholic HCV patients. (*A*) NS5A protein expression was assessed by immunoblot analysis in liver protein extracts from stroke patients with normal livers and HCV patients without or with the history of alcoholism compared with NS5A Tg mouse livers. (*B*) Densitometry results of NS5A proteins normalized by β-actin are shown. HCV patients with or without alcoholism had comparably induced NS5A protein expression at the level approximating one third of the expression observed in NS5A Tg mice. (*C–F*) Liver sections from healthy livers from stroke patients and hepatitis C patients with or without alcoholism were stained for TLR4, phospho-JNK, and phospho-IκB. Note colocalization signals (merged images) for TLR4 with phosphor-JNK or phosphor-IκB were increased in nonalcoholic and alcoholic HCV patients. (*F*) Negative control staining of liver sections from an HCV patient using isotype nonimmune antibody.

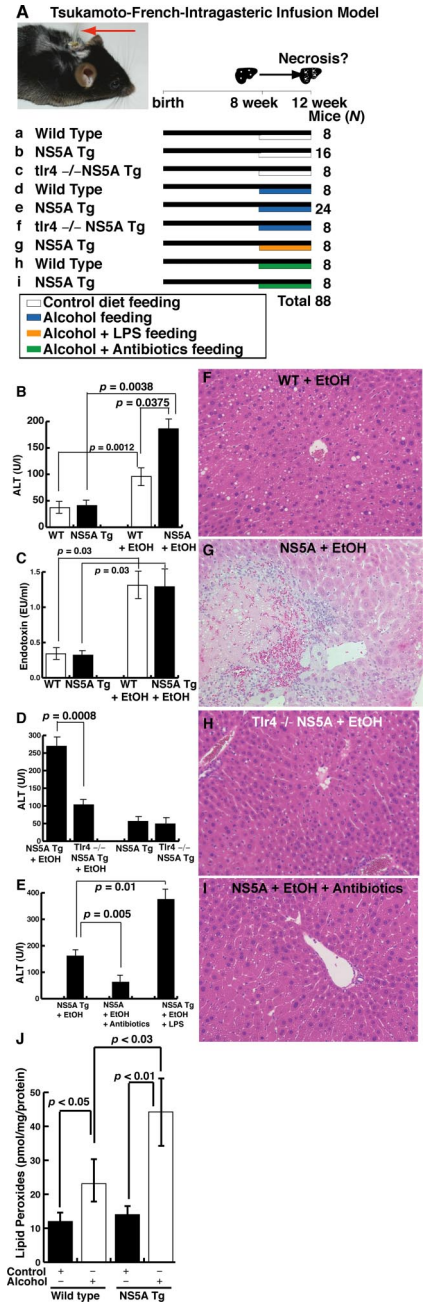

Fig. S3. NS5A-induced TLR4 triggers alcohol-induced submassive necrosis and enhanced oxidant damage. (*A*) A schematic diagram depicting the experimental design of 4-week intragastric ethanol feeding of different genetic mice. (*B*) Serum ALT of alcohol-fed NS5A transgenic mice in NS5A Tg and WT mice. Note a more accentuated increase in serum ALT levels in NS5A mice compared with WT mice after 4 weeks of intragastric ethanol infusion. (*C*) Plasma endotoxin levels in ethanol-fed NS5A Tg and WT mice compared with these mice before 4-wk intragastric infusion of ethanol. Plasma endotoxin levels were equally elevated in ethanol-fed WT and NS5A mice. (*D*) Increased serum ALT levels in ethanol-fed NS5A mice were reduced in TLR4$^{-/-}$NS5A mice fed ethanol. (*E*) Serum ALT of alcohol-fed NS5A transgenic mice in the presence or absence of antibiotics or enteral LPS treatment. Antibiotics treatment kills gut bacteria, which is a source of endotoxin. Antibiotic treatment attenuated and intragastric LPS administration augmented an increase in serum ALT levels in NS5A mice fed ethanol. (*F–I*) Submassive coagulative necrosis and intense inflammation were noted in the livers from ethanol-fed NS5A mice (*G*) but not from ethanol-fed WT mice (*F*). Note aggravated alcoholic liver pathology seen in NS5A mice was prevented in Tlr4$^{-/-}$NS5A mice and NS5A mice given antibiotics (*H* and *I*). (*J*) Lipid peroxides (4-hydroxyalkenals and malondialdehyde) of livers from wild-type and NS5A Tg mice were analyzed by a commercial assay (LPO-586; OXIS International Inc.). Note alcohol feeding significantly increased hepatic lipid peroxide content in wild-type mice, and this increase was significantly more accentuated in NS5A Tg mice.

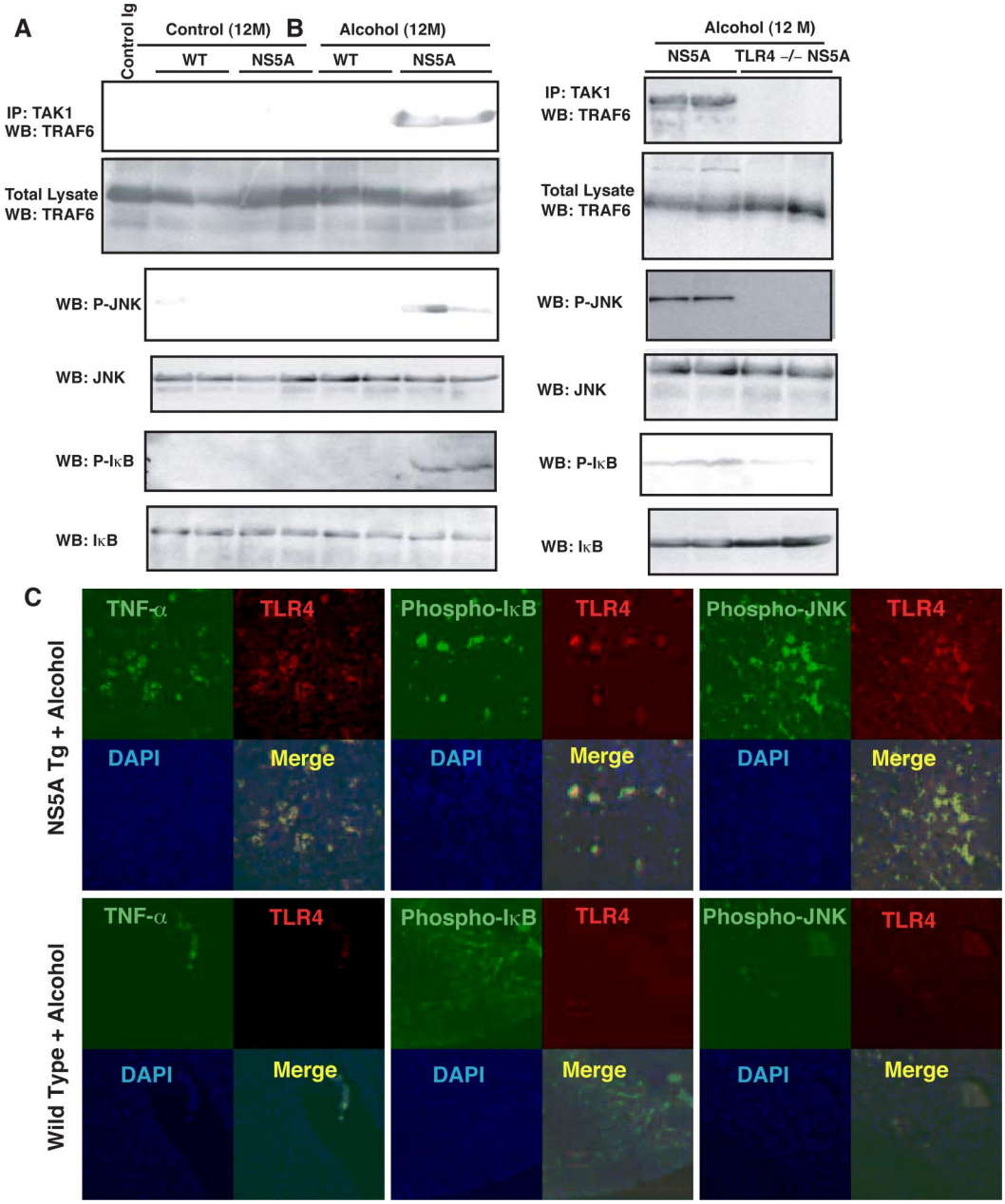

Fig. S4. Long-term alcohol feeding causes enhanced activation of TLR4 signaling in NS5A Tg mice. (*A*) Alcohol feeding for 12 months resulted in accentuated TLR4 signaling, as demonstrated by enhanced interaction of TAK1 with TRAF6 and increased expression of phosphor-JNK and phosphor-IκB in the livers of NS5A Tg mice compared with alcohol-fed wild-type (WT) mice or WT and NS5A Tg mice fed a control diet. (*B*) Accentuated TLR4 signaling in the livers of alcohol-fed NS5A Tg mice was completely prevented by TLR4 deficiency ($Tlr4^{-/-}$NS5A). (*C*) Liver cyosections from NS5A Tg and WT mice fed alcohol for 12 months were stained for TLR4, TNF-α, phospho-IκB, and phospho-JNK. Note increased colocalization of TLR4 staining with the staining for TNF-α, phospho-IκB, and phospho-JNK in alcohol-fed NS5A Tg mice compared with alcohol-fed WT mice.

A **NS5A + Alcohol vs. Wild type + Alcohol (Microarray)**

Function	Gene name	Fold change
Stem cell	Nanog homeobox (Nanog)	5.1
Cytokine	Interferon alpha 4 (Ifna4)	5.3
Chromatin remodeling	Absent, small, homeotic discs 1 (ASH1): Trithorax group	0.02
	Absent, small, homeotic discs 1 (ASH2): Trithorax group	0.07
Transcription factor	Homeo box D12 (HoxD12)*	0.42
	Homeo box C6 (HoxC6)*	0.45
	Homeo box C8 (HoxC8)	0.45
	Homeo box A9 (HoxA9)	0.48
	Myomesin M2 (MyoM2)	0.042
	Myomesin Z1 (MyoZ1)	0.13
	Myomesin Z2 (MyoZ2)	0.27
	Myogenic differentiation D1 (MyoD1)*,#	0.42
	Sine oculis-related homeobox 6 homologue (Six6)#	0.23
	Early B-cell factor 3 (Ebf3)#	0.37
	Paired box gene 6 (Pax6)#	0.42
	Inactive X specific transcripts (Xist)	0.41
	Forkhead box L1 (FoxL1)#	0.28
	Forkhead box O4 (FoxO4)	0.35
	Forkhead box D3 (FoxD3)*	0.44
	IKAROS family zinc finger 4 (Ikzf4)	4.7
Apoptosis	B-cell leukemia/lymphoma 2 related protein A1a (Bcl2a1a)	7.3
	B-cell CLL/lymphoma 11A (zinc finger protein) (Bcl11a)	4.3
Chromosome	Telomerase meintenace 2 (TEL2)	0.0036
	SWI/SNF related matrix associated	0.0034
Metabolism	Metallothionein 2 (Mtt2)	4.0
Membrane	Amyloid beta (A4) precursor protein (App)	9.5
	Serum amyloid A 2 (Saa2)	9.4

*: Promoter sequence has Nanog binding region
#: Promoter sequence has SUZ12 binding region

B **NS5A + Alcohol vs. Wild type + Alcohol (Microarray)**

		Fold change
glycosylation dependent cell adhesion molecule 1	Glycam1	125.5
intelectin 1 (galactofuranose binding) /// similar to Intelectin-1	Itln1 /// LOC640587	33.1
homeo box D9	Hoxd9	25.2
IKAROS family zinc finger 4	Ikzf4	18.1
similar to Ig heavy chain V region 108A precursor /// similar t	LOC100048770	16.7
peptidylprolyl isomerase (cyclophilin) like 5	Ppil5	15.5
G protein-coupled receptor 137B	Gpr137b	12.8
immunoglobulin mu binding protein 2	Ighmbp2	11.3
kallikrein 1-related peptidase b3	Klk1b3	10.5
somatostatin receptor 3	Sstr3	10.0
amyloid beta (A4) precursor protein	App	9.5
serum amyloid A 2	Saa2	9.4
hyaluronoglucosaminidase 1	Hyal1	8.8
deoxyribonuclease 1-like 3	Dnase1l3	8.7
cDNA sequence BC006965	BC006965	8.7
keratin 14	Krt14	8.6
immunoglobulin heavy chain complex /// Immunoglobulin he	Igh /// Ighg	8.5
S100 calcium binding protein G	S100g	8.1
tweety homolog 1 (Drosophila)	Ttyh1	8.0
cDNA sequence U46068	U46068	7.6
microrchidia 1	Morc1	7.6
granzyme G	Gzmg	7.4
tripartite motif protein 16	Trim16	7.4
B-cell leukemia/lymphoma 2 related protein A1a /// B-cell leu	Bcl2a1a /// Bcl2a1b	7.3
ankyrin repeat domain 1 (cardiac muscle)	Ankrd1	7.2
lipocalin 2	Lcn2	7.2
mitogen activated protein kinase 8 interacting protein 1	Mapk8ip1	7.0
involucrin	Ivl	6.9
centromere protein E	Cenpe	6.8
Immunoglobulin heavy chain 6 (heavy chain of IgM)	Igh-6	6.8
testis expressed gene 18	Tex18	6.7
high-mobility group box 4	Hmgb4	6.6
cysteine-rich secretory protein 2	Crisp2	6.3
cysteine-rich protein 3	Crip3	6.2
gonadotropin releasing hormone receptor	Gnrhr	6.0
mitogen activated protein kinase 10	Mapk10	6.0
G protein-coupled receptor 44	Gpr44	6.0
regenerating islet-derived 3 alpha	Reg3a	5.9
mitochondrial ribosomal protein L41	Mrpl41	5.7
protocadherin beta 10	Pcdhb10	5.6
angiopoietin-like 2	Angptl2	5.5
pancreatic lipase-related protein 2	Pnliprp2	5.5
lin-28 homolog (C. elegans)	Lin28	5.3
interferon alpha 4	Ifna4	5.3
olfactory receptor 1507	Olfr1507	5.2
expressed sequence AA522020	AA522020	5.1
Nanog homeobox	Nanog	5.1
chloride channel calcium activated 3	Clca3	5.0
phytanoyl-CoA hydroxylase interacting protein-like	Phyhipl	5.0
zinc finger protein 706	LOC100042741	5.0
retinal pigment epithelium 65	Rpe65	5.0
expressed sequence AI586015	AI586015	4.9
bireqional cell adhesion molecule-related	Boc	4.9
a disintegrin and metallopeptidase domain 3 (cyritestin)	Adam3	4.9
forkhead box B2	Foxb2	4.7
receptor tyrosine kinase-like orphan receptor 1	Ror1	4.7
annexin A2	Anxa2	4.7
LIM homeobox protein 9	Lhx9	4.6
expressed sequence BB001228	BB001228	4.6
expressed sequence C76554	C76554	4.5
acyl-CoA synthetase bubblegum family member 1	Acsbg1	4.4
Nephronectin	Npnt	4.4
sialic acid binding Ig-like lectin 5	Siglec5	4.4
tweety homolog 1 (Drosophila)	Ttyh1	4.3
syntaxin 1B2 /// syntaxin 1B1	Stx1b1 /// Stx1b2	4.3
CD209e antigen	Cd209e	4.3
spermatid perinuclear RNA binding protein	Strbp	4.3
B-cell CLL/lymphoma 11A (zinc finger protein)	Bcl11a	4.3
expressed sequence C77545	C77545	4.3
histocompatibility 28	H28	4.2
transmembrane protein 45a	Tmem45a	4.2
zona pellucida 3 receptor	Zp3r	4.2
Immunoglobulin heavy chain (gamma polypeptide)	Ighg	4.2
beaded filament structural protein in lens-CP94	Bfsp1	4.1
ubiquitin carboxyl-terminal esterase L4	Uchl4	4.1
Down syndrome cell adhesion molecule-like 1	Dscaml1	4.1
inhibitor of DNA binding 4 /// similar to Id4	Id4 /// LOC1000455	4.1
DAZ interacting protein 1	Dzip1	4.1
metallothionein 2	Mt2	4.0
cyclin G associated kinase	Gak	4.0
zinc finger protein 61	Zfp61	4.0

		Fold change
homeo box A9	Hoxa9	0.4865
forkhead box N4	Foxn4	0.4760
homeo box C8	HoxC8	0.4595
homeo box C6	Hoxc6	0.4572
forkhead box D3	Foxd3	0.4478
homeo box D12	Hoxd12	0.4228
myogenic differentiation 1	Myod1	0.4225
myomesin 1	Myom1	0.4160
early B-cell factor 3	Ebf3	0.3721
transferrin receptor	Tfrc	0.3714
granzyme N	Gzmn	0.3676
v-Ki-ras2 Kirsten rat sarcoma viral oncogene homolog	Kras	0.3650
forkhead box O4	Foxo4	0.3557
interferon regulatory factor 7	Irf7	0.3515
NADPH oxidase 4	Nox4	0.3325
2'-5' oligoadenylate synthetase 1D/1E	Oas1d/1e	0.3192
early B-cell factor 2	Ebf2	0.2564
G protein-coupled receptor 98	Gpr98	0.2469
Shc SH2-domain binding protein 1	Schbp1	0.2096
zinc finger CCCH type containing 3	Zc3h3	0.2495
cell cycle exit and neuronal differentiation 1	Cend1	0.2494
DnaJ (Hsp40) homolog	subfamily A	0.2493
calcium-binding tyrosine-(Y)-phosphorylation regulated	Cabyr	0.2487
RIKEN cDNA 1700120B22 gene	1700120B22Rik	0.2474
G protein-coupled receptor 98	Gpr98	0.2469
ATPase	Na+/K+ transporting	0.2469
gap junction membrane channel protein alpha 5	Gja5	0.2462
cholecystokinin A receptor	Cckar	0.2434
Wnt inhibitory factor 1	Wif1	0.2422
thyroglobulin	Tg	0.2419
G-protein-coupled receptor 50	Gpr50	0.2419
RIKEN cDNA 2310039E09 gene	2310039E09Rik	0.2413
leucine zipper protein 1	Luzp1	0.2380
alpha fetoprotein	Afp	0.2378
chemokine (C-X-C motif) ligand 13	Cxcl13	0.2362
sine oculis-related homeobox 6 homolog (Drosophila)	Six6	0.2361
proteolipid protein (myelin) 1	Plp1	0.2321
serine (or cysteine) peptidase inhibitor	clade F	0.2315
nuclear transcription factor-Y alpha	Nfya	0.2284
lipocalin 13	Lcn13	0.2260
DEAH (Asp-Glu-Ala-His) box polypeptide 9	Dhx9	0.2255
stathmin-like 2	Stmn2	0.2255
ubiquitin D	Ubd	0.2209
ribosomal protein L3-like	Rpl3l	0.2203
galactosylceramidase	Galc	0.2185
proteasome (prosome	macropain) subunit	0.2181
RIKEN cDNA 3110043J09 gene	3110043J09Rik	0.2166
cytochrome c oxidase	subunit VI a	0.2111
coiled-coil domain containing 53	Ccdc53	0.2102
kinesin family member 5C	Kif5c	0.2100
Shc SH2-domain binding protein 1	Shcbp1	0.2096
hypothetical LOC667597	LOC667597	0.2090
proteasome (prosome	macropain) subunit	0.2072
leiomodin 2 (cardiac)	Lmod2	0.2051
engrailed 1	En1	0.2043
RIKEN cDNA C330027C09 gene	C330027C09Rik	0.2031
expressed sequence AI451617	AI451617	0.2018
similar to MAS1 oncogene	LOC100048871	0.2006
doublecortin	Dcx	0.2004
trophoblast glycoprotein	Tpbg	0.1983
caspase 14	Casp14	0.1979
teratocarcinoma-derived growth factor /// similar to cripto	LOC10004	0.1947
chloride channel	nucleotide	0.1835
chemokine (C-X-C motif) ligand 13	Cxcl13	0.1830
casein alpha s2-like A	Csn1s2a	0.1823
sex determining region of Chr Y	Sry	0.1712
RAD51 associated protein 1	Rad51ap1	0.1668
ATP-binding cassette	sub-family	0.1630
VATPase	H+ transpx	0.1626
ATPase	H+ transpx	0.1621
proteasome (prosome	macropain) 26S subunit	0.1500
proteasome (prosome	macropain) subunit	0.1496
interferon-induced protein 44	Ifi44	0.0915
NADH dehydrogenase (ubiquinone) 1	subcomplex unknown	0.0598
succinate dehydrogenase complex	subunit C	0.0588
DnaJ (Hsp40) homolog	subfamily C	0.0557
potassium voltage-gated channel	shaker-related subfamily	0.0496
potassium channel	subfamily K	0.0495
lectin	galactose	0.0474
nuclear receptor subfamily 4	group A	0.0083
procollagen	type IV	0.0074
amyloid beta (A4) precursor protein-binding	family A	0.0073
nuclear factor of activated T-cells	cytoplasm	0.0072
dynein	axonemal	0.0037
TEL2	telomere maintenance 2	0.0026
golgi associated	gamma adaptin ear containing	0.0020
carbamoyl-phosphate synthetase 2	aspartate I	0.0019
glutamate receptor	ionotropic	0.0018
melanoma antigen	family L	0.0011
calcium channel	voltage-de	0.0010
potassium voltage-gated channel	Isk-related	0.0000
tyrosine kinase	non-recep	0.0005
protein tyrosine phosphatase	receptor type	0.0005
SAM domain	SH3 domain and nuclear localization signals	0.0004

Fig. S5. Differentially regulated genes in the livers of NS5A Tg mice fed alcohol for 12 months. DNA microarray analysis was performed in the livers of NS5A Tg mice and wild-type mice fed alcohol for 12 months as described in *SI Methods*. (*A*) This list summarizes differentially regulated genes in alcohol-fed NS5A mouse livers for different functional groups. Of note is the 5.1-fold induction of the stem cell marker Nanog. (*B*) A partial list of genes up-regulated by more than 4-fold or down-regulated by more than 2-fold in the livers of alcohol-fed NS5A Tg mice compared with alcohol-fed wild-type mice.

Table S1. Liver histological grading of NS5A Tg mice with or without TLR deficiency after 4-week alcohol feeding

Mouse	Diet	Fatty liver (0–4+)	Spotty necrosis (0–2+)	Submassive necrosis (0–2+)	Inflammation (0–2+)
WT	Ethanol	2.8 ± 0.7	0	0	0.5 ± 0.3
NS5A Tg	Ethanol	1.9 ± 0.6	0.5 ± 0.2	1.5 ± 0.4†	1.4 ± 0.6†
Tlr4 $^{-/-}$ NS5A Tg	Ethanol	1.0 ± 0.3‡	0.1 ± 0.2	0.1 ± 0.1‡	0.2 ± 0.2‡
NS5A Tg	Ethanol plus antibiotics	1.9 ± 0.3	0.3 ± 0.4	0.4 ± 0.1‡	0.3 ± 0.4‡
NS5A Tg	Ethanol plus LPS	2.2 ± 0.5	1.8 ± 0.5	1.6 ± 0.2‡	1.7 ± 0.7‡

Fatty liver: 2+, 25≈50% heaptocytes with fat; 3+, 50≈75% with fat; 4+, >75% with fat. Submassive necrosis/inflammation: 1+, lesions encompassing less than one third acinus; 2+, lesions larger than whole acini.

†$P < 0.05$ compared with WT.

‡$P < 0.05$ compared with respective ethanol diet-fed NS5A Tg mice.

Table S2. Disruption of *Tlr4* prevents tumor development in NS5A Tg mice fed the alcohol diet for 12 months

Mouse	Diet	N	Tumor, %	Survival, %	Daily consumption, mL/mouse	Serum TNF-α, pg/mL	Body weight, g		Liver weight, g	Ratio of liver to body
							Begin	End		
WT	Control	22	0	86	17.2 ± 3.4	3 ± 1	23.8 ± 2.1	33.0 ± 2.1	1.3 ± 0.3	3.9
Tlr4$^{-/-}$	Control	24	0	87	18.1 ± 3.1	4 ± 2	23.9 ± 2.2	33.5 ± 2.3	1.2 ± 0.2	3.7
NS5A Tg	Control	41	0	86	18.1 ± 4.1	4 ± 3	24.7 ± 2.6	34.1 ± 3.7	1.6 ± 0.3	4.5
Tlr4$^{-/-}$NS5A Tg	Control	18	0	83	17.6 ± 3.6	3 ± 2	23.5 ± 1.7	35.9 ± 3.5	1.5 ± 0.4	3.9
WT	Ethanol	21	0	67	15.3 ± 2.8	12 ± 5[†]	25.9 ± 2.8	31.2 ± 2.5	1.5 ± 0.5	5.2
Tlr4$^{-/-}$	Ethanol	26	0	69	16.1 ± 4.4	7 ± 5	23.7 ± 2.4	29.2 ± 3.6	1.5 ± 0.7	3.9
NS5A Tg	Ethanol	42	23[‡]	62	15.7 ± 3.0	24 ± 8[§]	24.3 ± 3.3	29.5 ± 3.9	1.9 ± 0.8	6.7
Tlr4$^{-/-}$NS5A Tg	Ethanol	19	0	63	16.3 ± 4.0	9 ± 6[¶]	24.5 ± 2.7	30.2 ± 3.8	1.7 ± 0.5	5.4

The percentage of males and female animals in different experimental groups ranged 45–55% males and 45–53% females. The tumor incidences in the 2 sexes in ethanol-fed TLR4 Tg mice were 13% for females and 36% for males ($P > 0.05$, χ^2 test).

[†]$P < 0.05$ compared with respective control diet-fed groups.

[‡]$P < 0.006$ compared with all other groups.

[§]$P < 0.05$ compared with ethanol-fed WT.

[¶]$P < 0.02$ compared with ethanol-fed Tlr4$^{-/-}$NS5A.

Table S3. Sex difference of tumor development in NS5A Tg mice fed the alcohol diet for 12 months

Mouse	Diet	N	Tumor, %	Survival, %	Sex, n: M/F	Survived mice, n: M/F	Tumor-bearing mice, n (%): M/F
WT	Ethanol	21	0	68	21/20	15/13	0/0
NS5A Tg	Ethanol	42	23[†]	62	19/23	11/15	4 (36)/2 (13)[‡]

[†] $P < 0.006$, Student's t test was performed to calculate statistical significance in comparison to those of WT mice.
[‡] $P = 0.736$, χ^2 test was performed to compare incidence of tumor development in sex difference, showing no statistical sex difference.